

REDUCED INTERFERENCE TIME-FREQUENCY REPRESENTATIONS AND SPARSE RECONSTRUCTION OF UNDERSAMPLED DATA

Yimin D. Zhang[†], Moeness G. Amin[†], and Braham Himed[‡]

[†] Center for Advanced Communications, Villanova University, Villanova, PA 19085, USA

[‡] RF Technology Branch, Air Force Research Lab (AFRL/RVMD), WPAFB, OH 45433, USA

ABSTRACT

In this paper, we examine the time-frequency representation (TFR) and sparse reconstruction of non-stationary signals in the presence of missing data samples. These samples lend themselves to missing entries in the instantaneous auto-correlation function (IAF) which, in turn, induce artifacts in the time-frequency distribution and ambiguity function. The artifacts are additive noise-like and, as such, can be mitigated by using proper time-frequency kernels. We show that the sparse signal reconstruction methods applied to the time-lag domain improve the TFR over the direct application of Fourier transform to the IAF. Additionally, the paper demonstrates that the use of signal-adaptive kernels provides superior performance compared to data-independent kernels when missing data are present.

Index Terms— Time-frequency analysis, missing data sample, sparse signal reconstruction, compressive sensing, non-stationary signals.

1. INTRODUCTION

Spectrum estimation and waveform reconstruction in the presence of missing data samples have broad applications in astronomy, seismology, paleoclimatology, and genetics [1, 2]. Missing data may be a consequence of removal of data samples contaminated by impulsive noise, or a result of intentional undersampling to enable digital signal processing of wideband signals and to reduce hardware complexity. A large class of non-stationary signals, particularly those with instantaneous narrowband waveforms, such as frequency-modulated (FM) signals with time-varying instantaneous frequencies (IFs), are widely used in the area of communications, radar systems, and biomedical applications [3]. For this type of signals, it is advantageous to use time-frequency representations (TFRs) to characterize the local signal behavior and determine the signal instantaneous frequency laws, even when many of the data samples are missing.

In this paper, we examine the effect of missing data on time-frequency distribution (TFD) performance and joint-variable representations. In particular, we consider the three domains of time-frequency, time-lag, and lag-frequency,

which respectively define TFD, instantaneous auto-correlation function (IAF), and ambiguity function (AF). We analytically show that the missing data samples yields missing entries in the IAF following certain patterns related to the time indices of the missing data samples. On the other hand, missing data produce artifacts in the TFD and AF domains which resemble additive noise in the sense that they spread over the entire respective domains of joint-variable representations. These artifacts can be mitigated by applying time-frequency kernels. In particular, the paper demonstrates that the use of signal-adaptive kernels provides superior performance compared to data-independent kernels when missing data are present.

Furthermore, we show that the sparse signal reconstruction methods applied to the IAF improve performance over the direct application of Fourier transform to the IAF. Unlike the sparsity-based TFD reconstructions which are based on the two-dimensional (2-D) Fourier transform relationship between the AF and the TFDs [4, 5], in this paper, the TFD reconstruction is based on the one-dimensional (1-D) Fourier transform that relates the IAF and the TFD domains. The latter method embeds significantly lower complexity.

Notations. A lower (upper) case bold letter denotes a vector (matrix). $(\cdot)^*$ denotes complex conjugation. $E[\cdot]$ represents the statistical mean operation. $\mathcal{F}_x(\cdot)$ and $\mathcal{F}_x^{-1}(\cdot)$ respectively represent the discrete Fourier transform (DFT) and inverse DFT (IDFT) with respect to x , whereas $\mathcal{F}_2(\cdot)$ denotes a two-dimensional (2-D) DFT. $\|\cdot\|_1$ and $\|\cdot\|_2$ respectively denote the L_1 and L_2 norm operations. In addition, $\delta(t)$ and $\delta(t, \tau)$ respectively denote 1-D and 2-D Kronecker delta functions, and $\text{var}(\cdot)$ denotes the variance.

2. SIGNAL MODEL

Consider a discrete-time signal, $x(t), t = 1, \dots, T$, which comprises a single or multiple components of FM signals. Denote $r(t)$ as its observation data with N missing samples, where $0 \leq N < T$. The missing sample positions are assumed to be randomly and uniformly distributed over time. As such, $r(t)$ is the product of $x(t)$ and an “observation mask”, $R(t)$, i.e.,

$$r(t) = x(t) \cdot R(t), \quad (1)$$

where

$$R(t) = \begin{cases} 1, & \text{if } t \in \mathbb{S}, \\ 0, & \text{if } t \notin \mathbb{S}. \end{cases} \quad (2)$$

The work of Y. D. Zhang and M. G. Amin was supported in part by a subcontract with Dynetics, Inc. for research sponsored by the Air Force Research Laboratory (AFRL) under Contract FA8650-08-D-1303.

$\mathbb{S} \subset \{1, \dots, T\}$ is the set of observed time instants and its cardinality is $|\mathbb{S}| = T - N$. The observed waveform with missing samples can be expressed as the difference between the original waveform and the ‘‘missing samples’’, i.e.,

$$r(t) = x(t) - m(t), \quad (3)$$

where the missing data is expressed as

$$m(t) = x(t) \cdot M(t), \quad (4)$$

with $M(t) = X(t) - R(t)$ denoting the ‘‘missing data mask’’, and

$$X(t) = 1, \quad \forall t, \quad (5)$$

is an ‘‘all-pass’’ mask.

To facilitate the analysis, we express the missing data mask as

$$M(t) = \sum_{i=1}^N \delta(t - t_i), \quad t_i \notin \mathbb{S}. \quad (6)$$

Accordingly, the missing signal is expressed as

$$m(t) = x(t) \cdot M(t) = \sum_{i=1}^N x(t) \delta(t - t_i) = \sum_{i=1}^N x(t_i) \delta(t - t_i), \quad (7)$$

and the observed data with the missing samples is expressed as

$$r(t) = x(t) - m(t) = x(t) - \sum_{i=1}^N x(t_i) \delta(t - t_i). \quad (8)$$

3. TIME-FREQUENCY REPRESENTATIONS WITH MISSING DATA SAMPLES

3.1. Instantaneous Auto-correlation Function

The IAF of $x(t)$ is defined as

$$C_{xx}(t, \tau) = x(t + \tau) x^*(t - \tau), \quad (9)$$

where τ is the time lag.

From (1) and (9), the IAF of $r(t)$ is expressed as

$$C_{rr}(t, \tau) = C_{xx}(t, \tau) C_{RR}(t, \tau), \quad (10)$$

where $C_{RR}(t, \tau)$ is the IAF of the observation mask $R(t)$. To examine the effect of the missing data samples more clearly, we use $R(t) = X(t) - M(t)$ to obtain

$$C_{RR}(t, \tau) = C_{XX}(t, \tau) + C_{MM}(t, \tau) - C_{XM}(t, \tau) - C_{MX}(t, \tau), \quad (11)$$

where $C_{XX}(t, \tau)$ and $C_{MM}(t, \tau)$ are the IAF of $X(t)$ and $M(t)$, respectively, and $C_{XM}(t, \tau)$ and $C_{MX}(t, \tau)$ are two IAF cross-terms between $M(t)$ and $X(t)$. The difference in the mask IAF due to the missing data samples can be expressed as

$$C_D(t, \tau) = C_{XX}(t, \tau) - C_{RR}(t, \tau) = C_{XM}(t, \tau) + C_{MX}(t, \tau) - C_{MM}(t, \tau). \quad (12)$$

From the definitions, we obtain

$$\begin{aligned} C_{MM}(t, \tau) &= \sum_{i=1}^N \delta(t - t_i + \tau) \sum_{k=1}^N \delta(t - t_k - \tau) \\ &= \sum_{t_i \notin \mathbb{S}} \delta(t - t_i, \tau) + \sum_{\substack{t_i, t_k \notin \mathbb{S} \\ t_i - t_k > 0, \text{ even}}} \delta\left(t - \frac{t_i - t_k}{2}, \tau \pm \frac{t_i - t_k}{2}\right). \end{aligned} \quad (13)$$

The first term in the right-hand side includes the entries in the t -axis (i.e., $\tau = 0$), whereas the last term represents entries off the t -axis due to different missing data samples. The cross-term IAF $C_{XM}(t, \tau)$ is given by

$$\begin{aligned} C_{XM}(t, \tau) &= \sum_{i=1}^N X(t + \tau) \delta(t - t_i - \tau) \\ &= \sum_{i=1}^N \sum_{k=1}^T \delta(t - t_k, \tau - t_k + t_i), \end{aligned} \quad (14)$$

which is a straight line across all values of $t \in [1, T]$, where τ satisfies $\tau = t - t_i$ for all missing data sample positions $t_i \notin \mathbb{S}$. On the other hand, the cross-term IAF $C_{MX}(t, \tau)$ is symmetric to $C_{XM}(t, \tau)$ with respect to the t -axis, and is given by

$$\begin{aligned} C_{MX}(t, \tau) &= \sum_{i=1}^N \delta(t - t_i + \tau) X(t - \tau) \\ &= \sum_{i=1}^N \sum_{k=1}^T \delta(t - t_k, \tau + t_k - t_i), \end{aligned} \quad (15)$$

which is a straight line that satisfies $\tau = -t + t_i$ for all $t_i \notin \mathbb{S}$. Notice that the non-zero entries of $C_{MM}(t, \tau)$ are located at the positions where the two IAF cross-terms meet, thereby maintaining the value of $C_M(t, \tau)$ not to exceed 1.

In reality, the IAF is affected by the window effect due to zero-padding. The length of the rectangular window along the τ dimension depends on t and is expressed as

$$Q_\tau(t) = T - |T + 1 - 2t|, \quad t = 1, \dots, T. \quad (16)$$

By taking this into account, a T -sample function $1(t)$ would have $T^2/2$ non-zero entries if T is even, or $(T^2 + 1)/2$ entries if T is odd. Without loss of generality, we consider an even value of T hereafter. In this case, the number of unit-value entries of $C_D(t, \tau)$, in the presence of N missing data samples, can be well approximated as

$$\tilde{N} = NT - N^2/2. \quad (17)$$

This implies the same number of missing entries in $C_{rr}(t, \tau)$.

3.2. Wigner-Ville Distribution

The DFT of the IAF $C_{xx}(t, \tau)$ with respect to τ is the well-known Wigner-Ville distribution (WVD), which represents the time-frequency (TF) characteristics of the signal,

$$W_{xx}(t, f) = \mathcal{F}_\tau[C_{xx}(t, \tau)] = \sum_{\tau} C_{xx}(t, \tau) e^{-j4\pi f \tau}. \quad (18)$$

Note that 4π is used in the DFT instead of 2π because the time-lag τ takes an integer value. Because $C_{xx}(t, \tau)$ is conjugate symmetric and $C_{RR}(t, \tau)$ is symmetric with respect to τ , $C_{rr}(t, \tau)$ is conjugate symmetric with τ as well. As such, the WVD of the observed data, $W_{rr}(t, f) = \mathcal{F}_\tau[C_{rr}(t, \tau)]$, is real-valued.

Because the missing data sample positions are randomly and uniformly distributed, from the above discussion, the positions of the missing IAF entries can also be considered randomly and uniformly distributed over t and τ . Then, for a specific t , out of the $Q_\tau(t)$ non-zero samples of $C_{xx}(t, \tau)$, the number of missing entries in $C_{rr}(t, \tau)$ is

$$K_\tau(t) = \frac{\tilde{N}}{T^2/2} Q_\tau(t) = \frac{2NT - N^2}{T^2} Q_\tau(t). \quad (19)$$

Therefore, the number of the observed non-zero IAF samples for a specific t is obtained as

$$L_\tau(t) = Q_\tau(t) - K_\tau(t) = \frac{(T - N)^2}{T^2} Q_\tau(t). \quad (20)$$

We can express $W_{rr}(t, f)$ as

$$W_{rr}(t, f) = \sum_{\tau \in \mathcal{S}_\tau(t)} C_{xx}(t, \tau) e^{-j4\pi f \tau}, \quad (21)$$

where $\mathcal{S}_\tau(t)$ is the set of non-zero τ entries for a specific t with a cardinality of $|\mathcal{S}_\tau(t)| = L_\tau(t)$, and τ takes values between $-[Q_\tau(t) - 1]/2$ and $[Q_\tau(t) - 1]/2$.

Using the uniform distribution of the missing entries in t and τ , it is straightforward to verify that $E[W_{rr}(t, f)] = [L_\tau(t)/Q_\tau(t)]W_{xx}(t, f)$, i.e., $W_{rr}(t, f)$ is an unbiased estimator of $W_{xx}(t, f)$ for every t and f , subject to a scaling factor $\xi = L_\tau(t)/Q_\tau(t) = (T - N)^2/T^2$. Write $W_{rr}(t, f)$ as

$$W_{rr}(t, f) = W_{xx}(t, f) - W_d(t, f), \quad (22)$$

where $W_d(t, f) = W_{mx}(t, f) + W_{xm}(t, f) - W_{mm}(t, f)$ denotes the artifacts in the WVD due to the missing data samples. Then, from the above discussion, we obtain

$$E[W_d(t, f)] = \left(1 - \frac{L_\tau(t)}{Q_\tau(t)}\right) W_{xx}(t, f) = \frac{K_\tau(t)}{Q_\tau(t)} W_{xx}(t, f). \quad (23)$$

Because $W_{xx}(t, f)$ is deterministic, we can obtain the variance of $W_{rr}(t, f)$ as

$$\begin{aligned} \text{var}[W_{rr}(t, f)] &= \text{var}[W_d(t, f)] \\ &= E \left[|W_d(t, f)|^2 - \left(\frac{K_\tau(t)}{Q_\tau(t)}\right)^2 |W_{xx}(t, f)|^2 \right] \\ &= \sum_{\tau \notin \mathcal{S}_\tau(t)} |C_{xx}(t, \tau)|^2 - \frac{K_\tau(t)}{Q_\tau^2(t)} |W_{xx}(t, f)|^2. \end{aligned} \quad (24)$$

Specifically, when $x(t)$ is a mixture of P FM signals with amplitudes $a_i, i = 1, \dots, P$, we can simplify the above expression as

$$\text{var}[W_{xx}(t, f)] = K_\tau(t) \left[\sum_{i=1}^P |a_i|^2 - \frac{1}{Q_\tau^2(t)} |W_{xx}(t, f)|^2 \right]. \quad (25)$$

As such, the missing data samples yield spreading artifacts that are randomly distributed over the entire t - f domain, and the overall variance increases as the number of missing data samples increases. It is evident from the above expression that, for (t, f) points where $W_{xx}(t, f)$ is zero or insignificant, the variance is uniformly distributed over f , whereas the variance depends on t because of the zero-padding effect.

3.3. Ambiguity Function

The IDFT of the IAF $C_{xx}(t, \tau)$ with respect to t yields the AF, expressed as,

$$A_{xx}(\theta, \tau) = \mathcal{F}_t^{-1}[C_{xx}(t, \tau)] = \sum_t C_{xx}(t, \tau) e^{j2\pi\theta t}, \quad (26)$$

where θ is the frequency shift or Doppler. As such, the AF is mathematically very similar to the WVD. The exception is that, as the IAF is conjugate symmetric only with τ but not with t , the AF entries are in general complex. Rather, The AF entries are conjugate symmetric with respect to the origin.

We similarly define the window length along the t dimension, which is expressed as a function of τ ,

$$Q_t(\tau) = T - |2\tau|, \quad \tau = -(N/2) + 1, \dots, (N/2) - 1. \quad (27)$$

Out of the $Q_t(\tau)$ samples of $C_{xx}(t, \tau)$ for a specific value of τ , the number of missing entries in $C_{rr}(t, \tau)$ is

$$K_t(\tau) = \frac{\tilde{N}}{T^2/2} Q_t(\tau) = \frac{2NT - N^2}{T^2} Q_t(\tau). \quad (28)$$

We can similarly verify that $E[A_{rr}(\theta, \tau)] = (L_t(\tau)/Q_t(\tau)) A_{xx}(\theta, \tau)$, where $L_t(\tau) = Q_t(\tau) - K_t(\tau)$. That is, $A_{rr}(\theta, \tau)$ is an unbiased estimator of $A_{xx}(\theta, \tau)$ for every θ and τ , subject to the same scaling factor $\xi = L_t(\tau)/Q_t(\tau) = (T - N)^2/T^2$. The variance of $A_{rr}(\theta, \tau)$ is given as

$$\text{var}[A_{rr}(\theta, \tau)] = \sum_{t \notin \mathcal{S}_t(\tau)} |C_{xx}(t, \tau)|^2 - \frac{K_t(\tau)}{Q_t^2(\tau)} |A_{xx}(\theta, \tau)|^2, \quad (29)$$

where $\mathcal{S}_t(\tau)$ is the set of non-zero t entries for a specific τ with a cardinality of $|\mathcal{S}_t(\tau)| = L_t(\tau)$, and t takes values between 1 and T . The variance becomes

$$\text{var}[A_{rr}(\theta, \tau)] = K_t(\tau) \left[\sum_{i=1}^P |a_i|^2 - \frac{1}{Q_t^2(\tau)} |A_{xx}(\theta, \tau)|^2 \right] \quad (30)$$

when $x(t)$ is the mixture of P FM signals with magnitude $a_i, i = 1, \dots, P$, as described earlier.

As such, the missing data samples yield artifacts that randomly spread over the entire θ - τ domain, and the overall variance increases as the number of missing data samples increases. For (θ, τ) entries where $A_{xx}(\theta, \tau)$ is zero or insignificant, the variance is uniformly distributed over θ , whereas the variance depends on τ because of the zero-padding effect.

4. MITIGATION OF MISSING DATA ARTIFACTS USING TIME-FREQUENCY KERNELS

The effect of the artifacts due to missing data samples resembles that due to noise in the WVD and AF domains in the sense that they respectively spread over the entire t - f as well as the θ - τ regions. Therefore, such effect can be mitigated through a proper mask, or time-frequency kernel. This is a welcomed news because such kernels also mitigate undesired time-frequency cross-terms. As such, a less cluttered TFD can be expected with the suppression of both missing data artifacts and cross-terms. The best kernel in this case is one that only keeps the signal signature whereas the other regions are filtered out. One of the best choices for this purpose is the adaptive optimal kernel (AOK) [6], which is known to provide signal-adaptive filtering capability in the AF domain. Furthermore, to understand the difference between noise and the missing data samples, we also consider the Choi-Williams distribution (CWD) [7] as an example of non-adaptive kernels.

5. RECONSTRUCTION THROUGH L_1 -NORM BASED SIGNAL RECOVERY

When the signals are sparsely presented in the time-frequency domain, their TFDs can be reconstructed based on their sparsity. For notation convenience, we denote $\mathbf{c}_{\mathbf{xx}}^{[t]}$ as a vector that contains all IAF entries along the τ dimension corresponding to time t , and $\mathbf{d}_{\mathbf{xx}}^{[t]}$ as a vector collecting all the TFD entries for the same time t . Note that $\mathbf{c}_{\mathbf{xx}}^{[t]}$ may denote the original IAF, which corresponds to the WVD, or its smoothed version as a result of applying a kernel. Then, these two vectors are related by the IDFT with respect to f , expressed as

$$\mathbf{c}_{\mathbf{xx}}^{[t]} = \mathbf{G}_f \mathbf{d}_{\mathbf{xx}}^{[t]}, \quad \forall t, \quad (31)$$

where \mathbf{G}_f is a matrix performing the IDFT with respect to f .

Vector $\mathbf{c}_{\mathbf{xx}}^{[t]}$ may have missing entries due to missing data or because of the kernel. By removing the IAF entries with zero or negligible values, we can construct a vector $\tilde{\mathbf{c}}_{\mathbf{xx}}^{[t]}$, which becomes

$$\tilde{\mathbf{c}}_{\mathbf{xx}}^{[t]} = \tilde{\mathbf{G}}_f \mathbf{d}_{\mathbf{xx}}^{[t]}, \quad (32)$$

where $\tilde{\mathbf{G}}_f$ is the result after removing the corresponding rows from \mathbf{G}_f .

Because the signals are sparsely represented in the time-frequency domain, the non-zero entries of $\mathbf{d}_{\mathbf{xx}}^{[t]}$ can be reconstructed through sparse signal recovery techniques. The problem is formulated as

$$\min \|\mathbf{d}_{\mathbf{xx}}^{[t]}\|_1 \quad \text{s.t.} \quad \tilde{\mathbf{c}}_{\mathbf{xx}}^{[t]} - \tilde{\mathbf{G}}_f \mathbf{d}_{\mathbf{xx}}^{[t]} = 0, \quad \forall t. \quad (33)$$

In this paper, we use the orthogonal matching pursuit (OMP) [8] for each time instant. The reason of choosing the OMP is that it allows us to specify the number of non-zero entries (i.e., iterations) in each time instant.

6. SIMULATION RESULTS

For illustration purposes, we use a two-component FM signal, where the instantaneous phase laws of the two components are respectively expressed as,

$$\begin{aligned} \phi_1(t) &= 0.05t + 0.05t^2/T + 0.1t^3/T^2, \\ \phi_2(t) &= 0.15t + 0.05t^2/T + 0.1t^3/T^2, \end{aligned} \quad (34)$$

for $t = 1, \dots, T$, where T is chosen to be 128. The two FM components have the same power, and no noise is considered. The real-part waveform, WVD, AF, and IAF are depicted in Fig. 1. The WVD, AF, and IAF are shown in terms their magnitudes for better demonstration of the artifacts due to missing data samples. It is observed that the WVD shows clear cross-terms between the two components, as well as those between the same components due to the non-linear IF signatures. In addition, the total number of 8192 non-zero entries of the IAF has a diamond shape because of zero-padding.

Now, we consider the same waveform, but with a 50% (or 64) missing data samples that are randomly distributed over the 128 data samples. The waveform is shown in Fig. 2, where the missing data positions are marked with red dots. Per the analysis presented in Section 3, the IAF is a product of the original IAF and a mask function that nullifies its presence in a significant amount of entries. For this specific realization, the missing IAF entries due to the missing data samples is 6144 (which is 75% of the total entries of the original IAF), whereas the approximated value obtained from (17) is 6143.5. The average number of missing entries obtained from 100 independent trials is 6128.1.

It is evident in Fig. 2 that the missing IAF entries induce WVD and AF artifacts. The artifacts in the WVD are spread evenly over the frequency axis but has stronger presence in the central portion of the time axis due to the diamond shape of the IAF. They show certain periodicity because of the two signal components with parallel IF laws. These artifacts significantly obscure the proper identification of the time-frequency signatures in the WVD. Likewise, they are evenly distributed in the AF over the Doppler frequency, and shows higher presence when the time lag is close to zero.

The TFD obtained from the AOK is shown in Fig. 3(a) for 50% of missing data samples. It is evident that the AOK substantially mitigates the missing data artifacts. Because the AOK is originally designed for cross-term suppression, the resulting TFD shows a TFR with clear auto-term characteristics, even with 50% of missing data samples. The TFD obtained from the CWD is shown in Fig. 3(b) for the same 50% of missing data samples. A 7-sample Hamming window (approximately 1/20 of the entire data samples) is applied to θ , and a 43-sample Hamming window (approximately 1/3 of the entire data samples) is applied to τ . Because the CWD is not data-adaptive, it emphasizes the locality of the observed data when rejecting the artifacts due to missing data samples, yielding missing or weak TFD entries around missing data positions. This distinguishes the effect of the artifacts from that of additive noise.

Finally, we depict the TFDs results obtained from the observed data with missing samples by exploiting sparse signal reconstructions. It is clear that the signal is locally sparse

when considered through a window. The reconstructed TFDs using the OMP algorithm with few iterations are shown in Fig. 4. The result presented in Fig. 4(a) is obtained from the original IAF. Three iterations were allowed for each time instant to account for the cross-terms. The artifacts due to the missing data samples are still noticeable. On the other hand, Fig. 4(b) shows the results obtained from the IAF after applying the AOK, with two iterations used for each time instant. In this case, the reconstructed TFD shows a TFD with very little clutter.

7. CONCLUSIONS

We have examined the effect of missing data samples of non-stationary signals on the time-frequency representations and their sparse reconstructions. The Wigner-Ville distribution (WVD) of such observed signals is shown to be an unbiased estimator of the full-data WVD, and the estimated variance is analyzed. The artifacts due to the missing data samples are spread over the entire time-frequency domain and can be effectively suppressed by using proper time-frequency kernels. Waveform-adaptive kernels, such as the adaptive optimal kernel, demonstrated superior artifact suppression capability. Sparsity-based reconstruction techniques applied to interference-reduced distributions results in excellent time-frequency representations.

8. REFERENCES

- [1] A. Tarczynski and N. Allay, "Spectral analysis of randomly sampled signals: suppression of aliasing and sampler jitter," *IEEE Trans. Signal Proc.*, vol. 52, no. 12, pp. 3324–3334, Dec. 2004.
- [2] P. Babu and P. Stoica, "Spectral analysis of nonuniformly sampled data – a review," *Digital Signal Proc.*, vol. 20, pp. 359–378, 2010.
- [3] A. Papandreou-Suppappola (Editor), *Applications in Time-Frequency Signal Processing*, CRC Press, 2003.
- [4] P. Flandrin and P. Borgnat, "Time-frequency energy distributions meet compressed sensing," *IEEE Trans. Signal Proc.*, vol. 58, no. 6, pp. 2974–2982, June 2010.
- [5] Y. D. Zhang and M. G. Amin, "Compressive sensing in non-stationary array processing using bilinear transforms," in *Proc. IEEE Sensor Array and Multichannel Signal Processing Workshop*, Hoboken, NJ, June 2012.
- [6] D. L. Jones and R. G. Baraniuk, "An adaptive optimal-kernel time-frequency representation," *IEEE Trans. Signal Proc.*, vol. 43, no. 10, pp. 2361–2371, Oct. 1995.
- [7] H. I. Choi and W. J. Williams, "Improved time-frequency representation of multicomponent signals using exponential kernels," *IEEE Trans. Acoust., Speech, Sig. Proc.*, vol. ASSP-37, no. 6, pp. 862–871, June 1989.
- [8] J. A. Tropp and A. C. Gilbert, "Signal recovery from random measurements via orthogonal matching pursuit," *IEEE Trans. Info. Theory*, vol. 53, no. 12, pp. 4655–4666, 2007.

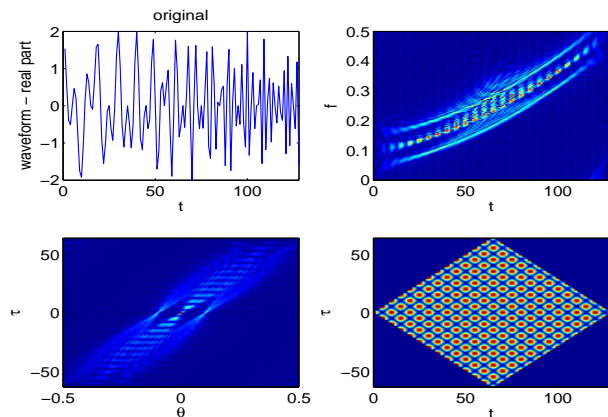


Fig. 1 Real-part waveform, WVD, AF, and IAF of the two-component signals without missing samples.

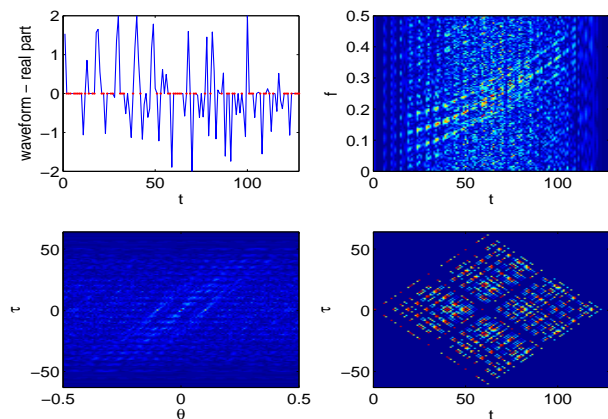


Fig. 2 Real-part waveform, WVD, AF, and IAF of the two-component signals with 50% of missing samples. The red dots in the waveform show the missing data positions.

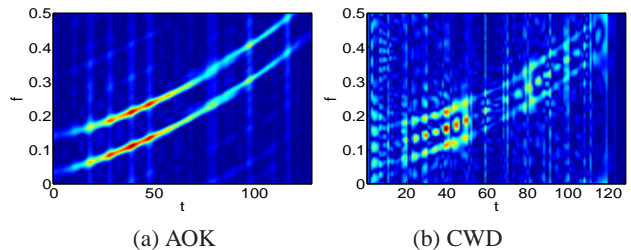


Fig. 3 TFDs obtained from AOK and CWD using data with 50% of missing samples.

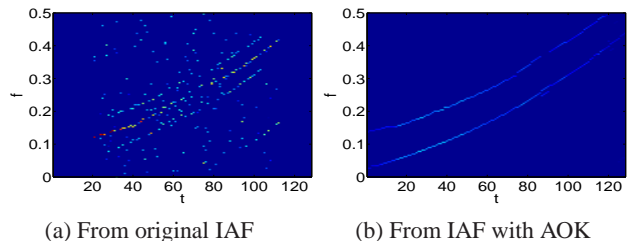


Fig. 4 TFDs reconstructed through OMP from the original and kernalled IAF using data with 50% of missing samples.